A Novel Miniaturized SSPP Based Low Pass Filter with Ultra-Wide-Stop-Band

Brij Kumar Bharti and Amar Nath Yadav, *Member, IEEE*

***Abstract*—This letter introduces a novel compact Spoof Surface Plasmon Polaritons (SSPPs) based low-pass filter (LPF) with ultra-wide out-of-band suppression. The filter design employs a single-layer printed circuit board, with the top layer incorporating metal gratings in a tilted slotted stub shape. The unique characteristic of the proposed SSPP LPF is the lower asymptotic frequency compared to traditional SSPP structures of equivalent size, making significant LPF miniaturization. The overall device size is $0.75\lambda_g \times 0.12\lambda_g$ (where λ_g denotes the guided wavelength). A lumped equivalent circuit model of the proposed SSPP unit cell is presented. Simulated results showcase excellent performance in the passband and impressive out-of-band suppression. A prototype of the proposed LPF is fabricated and measured to validate the design concept. Measured results closely align with simulation outcomes, revealing an insertion loss of 1.1 dB at the center frequency, reflection coefficient below -10 dB throughout the pass-band, and exceptional out-of-band rejection with an attenuation exceeding 30 dB for over 38 GHz.**

***Index Terms*—Spoof surface plasmon polaritons (SSPP), Transmission line (TL), Low Pass Filter, Band suppression**

I. Introduction

Surface plasmon polaritons (SPPs) are charge oscillations between the two surfaces of a metal and a dielectric material at the terahertz frequency region. SSPPs (spoof surface plasmon polaritons) are closely related to the SPPs, though their origins differ. SSPP was introduced using a periodic deformation on a metallic sheet in which the propagation of waves is similar to the SPP waves [1]. It can overcome the cross-talk or interference that occurs due to nearby transmission lines (TLs) in RF circuits and miniaturizing photonic and microwave components [2].

In [3], SSPP mode with a metal strip on a very thin dielectric substrate has been realized. An investigation has been done on the efficient broadband conversion of guided waves (quasi-TEM) supported by conventional transmission lines (microstrip and CPW lines) to SSPP waves supported by corrugated waveguides [4]. In [5], the arm of conventional double-sided SSPP has been tilted at various angles to reduce the vertical size of the structure. SSPP waveguides using T-shaped conductor branches, balanced coplanar stripline, meander-line, and modified conventional SSPP are designed to miniature the size [6]- [9]. Hybrid Substrate Integrated Waveguide (SIW)-SPP based wide band-pass filters (BPFs) have been discussed in [10]. In [11], analysis and comparison of single- and double-side grooves in SSPPs has been done. In [12], a compact SSPPs LPF with high-efficiency transmission and good out-of-band suppression is introduced. In [13], a folded structure SSPPs-based waveguide reduces longitudinal size while increasing transversal size is presented. Coplanar strip SSPP-based LPFs are presented for microwave and THz application in [14]- [16]. Utilization of the high-pass characteristics of SIW and the low-pass characteristics of SSPP has been employed in the design of bandpass filters in [17]-[18]. A controllable out-of-band rejection filter incorporating a short-circuited stub-loaded SSPP structure is introduced in [19]. In [20], a compact Filter using trident shape SSPP cells is designed with wide stopband suppression. A transition-free SSPP-based filter using an H-shaped and a bilateral T-shaped slot line is presented in [21]. Despite these efforts, the challenge of size miniaturization persists for plasmonic LPFs because of complex transitions and high asymptotic frequencies of SSPP unit cells. Also, limited attention has been given to out-of-band suppression in SSPP-based LPF designs. This article proposes a novel miniaturized SSPP-based LPF with ultra-wide-stop-band characteristics on a printed circuit board. Tilted metallic strips are used to miniaturize the SSPP unit cell. Slotting on those tilted strips has been done to reduce the asymptotic frequency and improve the out-of-band suppression. Further metallic straight strips are added on both sides of unit cells to improve band suppression.

II. Design and Analysis of SSPP Unit Cells

The characteristics of the supported SSPP mode, including cut-off frequency and propagation, depend on the unit cell's size and geometry. Dispersion characteristics, relating frequency and wavevector, describe the SSPP mode within the unit cell. Analyzing the dispersion diagram facilitates predicting the structure's cut-off frequency.

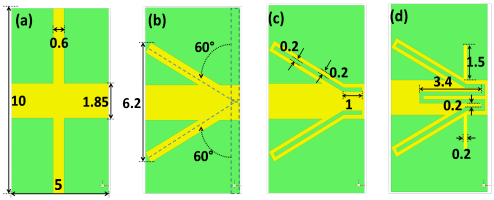

Fig. 1. Unit cell structures of (a) traditional SSPP unit cell, (b) tilted stub SSPP unit cell, (c) proposed unit cell-1, and (c) proposed unit cell-2. (dimensions unit: millimeter)

A. Evolution of proposed SSPP unit cell

The substrate used to design the SSPP structure is Roger 5880, with a relative permittivity of 2.2, a height of 0.501 mm, and a loss tangent of 0.0009. Initially, a traditional SSPP unit

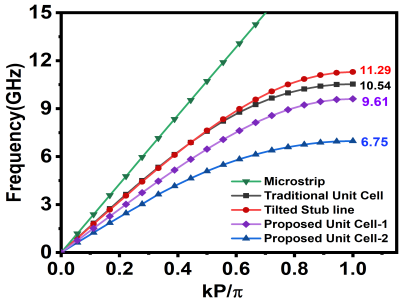

Fig. 2. Dispersion characteristics of different SSPP unit cells.

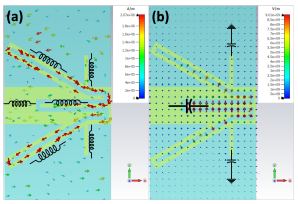

Fig. 3. Unit cell structures of (a) Current density in a unit cell, (b) E-field in a unit cell.

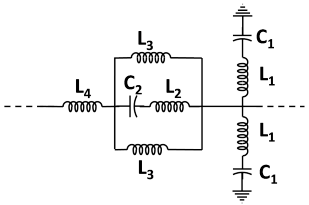

Fig. 4. Equivalent lumped circuit of proposed SSPP unit cell.($C_1 = 0.4pF$, $C_2 = 0.8pF$, $L_1 = 0.35nH$, $L_2 = 0.05nH$, $L_3 = 0.85nH$, and $L_4 = 0.7nH$)

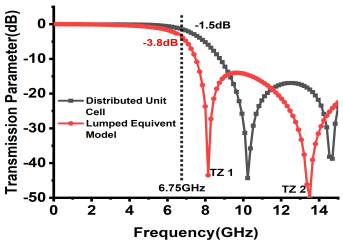

Fig. 5. Transmmision parameter of distributed and equivalent lumped circuit SSPP unit cell.

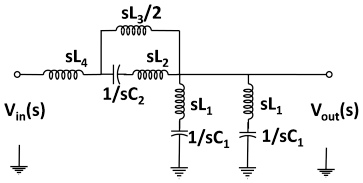

Fig. 6. LC equivalent lumped circuit of SSPP unit cell in laplace domain.

cell shown in Fig. 1(a), with dimensions of $10mm \times 5mm$ is designed, having an asymptotic frequency of 10.54 GHz. Subsequently, in the modified version presented in Fig. 1(b), the metal strips of the traditional SSPP cell are tilted by 60 degrees, effectively reducing the longitudinal size and resulting in an increased asymptotic frequency of 11.29 GHz. In Fig. 1(c), further adjustments are made to mitigate the asymptotic frequency, introducing slotting on the tilted metal strips, which brings the asymptotic frequency down to 9.61 GHz. The evolution continues in Fig. 1(d), where the slot between the tilted metal strips is modified and connected as one long slot. Additionally, 1.5mm metal strips are introduced on both sides, culminating in a substantially reduced frequency of 6.75 GHz. To attain an asymptotic frequency of 6.75 GHz, the transverse length of the traditional SSPP unit cell would need to be 16.2 mm, reflecting a 161.2% increase compared to the proposed SSPP unit cell-2. The eigen-mode analysis of unit cells is done using CST microwave studio. The dispersion curves of all different SSPP unit cells are presented in Fig.2.

B. Lumped Equivalent Circuit Model of Unit Cell.

Based on the observed behavior of current paths and electric field configurations within the unit cell, predictions for modeling inductance and capacitors and their series-parallel arrangements can be made. In Fig. 3, the unit cell's current density and E-field distribution reveal that the tilted arms exhibit a current flow from one side of the arm to the other, resembling an inductor. The straight metal strip can also be represented as an inductor in series with a capacitor. Moreover, the slot between the tilted arms forms two plates of a capacitor, as illustrated in Fig. 3. Fig. 4 presents the complete lumped circuit model of the proposed SSPP unit cell-2 structure. The values of capacitors and inductors are mentioned in the caption of Fig.4. In Fig. 5, transmission parameters for both the distributed and lumped equivalent unit cells are shown. Notably, at the asymptotic frequency of 6.75 GHz obtained from the dispersion diagram illustrated in Fig.2, the transmission parameter (S_{21}) values for the distributed and lumped equivalent unit cells are -1.5 dB and -3.8 dB, respectively. These values closely align with the 3 dB cutoff frequency of the LPF. This signifies the accurate modeling of the equivalent circuit, further supported by the close correspondence of the transmission parameter values with the LPF cutoff frequency. The transfer function (TF) can be calculated using the equivalent circuit in Fig. 6 to support the circuit modeling and its transmission zeros (TZs) analytically. The TF is given by:

$$\frac{V_{\text{out}}(s)}{V_{\text{in}}(s)} = \frac{s^4(a_1) + s^2(a_2) + 2}{s^4(b_1) + s^2(b_2) + 2} \tag{1}$$

where,

$$a_1 = L_1C_1L_2C_2 + L_1C_1L_3C_2 \tag{2}$$

$$a_2 = 2L_2C_2 + L_3C_2 + 2L_1C_1 \tag{3}$$

$$b_1 = L_1C_1L_3C_2 + 2L_1C_1L_2C_2 + 2L_3L_4C_1C_2 + 4L_4C_1L_2C_2 \tag{4}$$

$$b_2 = 2L_2C_2 + L_3C_2 + 2L_1C_1 + 2C_1L_3 + 4C_1C_4 \tag{5}$$

To find the TZs for this TF, solution of equation 6 is required.

$$\frac{V_{\text{out}}(s)}{V_{\text{in}}(s)} = 0 \Rightarrow s^4(a_1) + s^2(a_2) + 2 = 0 \tag{6}$$

After solving Equation (6), and putting inductances and capacitances values given in Fig.4 caption, there will be two positive and two negative values of s. Considering only positive values, in this case, $s_1 = j8.45 \times 10^{10}$ and $s_2 = j5.12 \times 10^{10}$.

Since, $s = j2\pi f \Rightarrow f_1 = 8.1$ GHz and $f_2 = 13.4$ GHz. f_1 and f_2 are the TZ points shown in Fig. 5.

III. Design And Simulation of Low Pass Filter

A. LPF using Traditional SSPP cell

To demonstrate the issues related to large transversal size and harmonics in an LPF constructed using traditional SSPP unit cells, a structure has been designed and depicted in Fig. 7. To maintain the cut-off frequency of 6.75 GHz, the transversal size of metal strips has been increased to 16.2 mm. However, this increased size needs to be miniaturized to enable the design of compact RF/microwave circuits. To achieve impedance matching in the passband, tapering has been applied to the lengths of the metal strips. Simulated S-parameters are presented in Fig. 8. Figure 8 shows that the out-of-band suppression is very poor, and multiple harmonics are occurring, which need to be suppressed for high-performance applications.

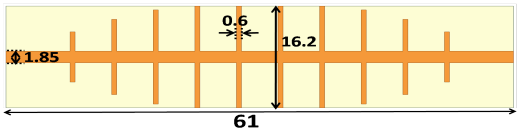

Fig. 7. Schematic configuration of traditional SSPP LPF.(unit: millimeter)

B. LPF Design using Proposed SSPP cell

Based on the proposed unit cell-2, an LPF is designed, which is demonstrated in Fig. 9. The metal footprint in the transversal direction is reduced to 6.2mm, decreasing the overall device size by 61.7% compared to the filter in Fig.7.

The simulated S-parameter results are presented in Fig. 10, demonstrating excellent performance both within and outside the passband. Within the passband, ranging from 0 to 6.77 GHz, the return loss remains below 15 dB, and the insertion loss is merely 0.27 dB at the center frequency. The 3 dB cut-off frequency of this filter closely aligns with the asymptotic frequency of the unit cell employed in its design. Additionally, an ultra-wideband out-of-band suppression, spanning from 7.5

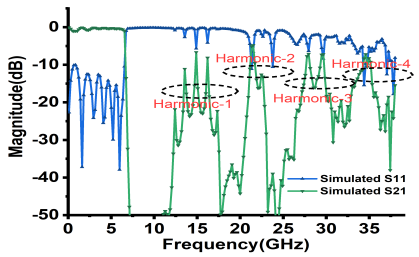

Fig. 8. Simulated S-Parameter of traditional SSPP filter.

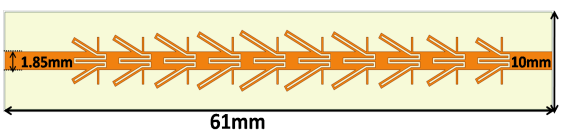

Fig. 9. Schematic configuration of proposed LPF

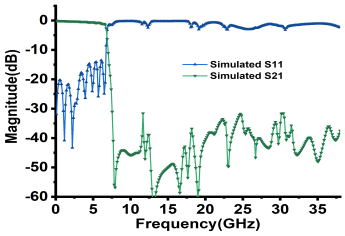

Fig. 10. Simulated S-Parameters of the proposed filter.

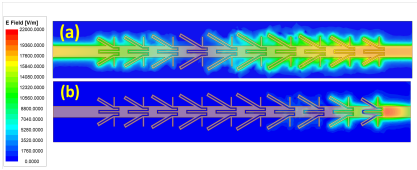

Fig. 11. Distributions of electric field for frequencies (a) 1 GHz and (b) 10 GHz.

to 38 GHz, is evident in Fig. 10, with attenuation exceeding 30 dB. Figure 11 presents the electric field distributions of the SSPP-based LPF at two frequencies, 1 GHz and 10 GHz, falling in the passband and stopband, respectively. At 1 GHz, the electric fields are prominently concentrated on the metallic strips, indicative of the transmission through the SSPP waveguide facilitated by the propagation of the excited SSPP mode. Conversely, at 10 GHz, the electric fields encounter obstruction at the transition region characterized by high electric field intensity, resulting in effective blocking and confinement within the stopband.

IV. Experimental Results

To validate the feasibility of the proposed design, prototype fabrication of the SSPP-based LPF has been done. The top view of the fabricated SSPP filter is illustrated in Figure 12, with the backs covered by copper, acting as the ground. As depicted in Fig. 13, measured results encompass S-parameters, exhibiting agreement with simulated outcomes. The fabricated sample demonstrates excellent passband characteristics, including robust Return Loss (RL) exceeding 10 dB, with low Insertion Loss (IL) of 1.1 dB. Furthermore, the roll-off rate at the band edge remains favorable. Notably, the filter's performance experiences a slight deterioration, possibly due to tolerance in measurement and fabrication of the filter potentially attributed to external disturbances, as no shielding cavities were employed during measurements. Performance comparisons with prior works, presented in Table I, underscore the merits of the proposed SSPP, showcasing compact

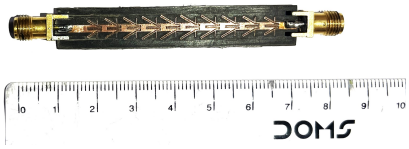

Fig. 12. Photograph of fabricated SSPP LPF.

TABLE I
COMPARISONS WITH PREVIOUSLY PUBLISHED STUDIES

Ref.	3dB Pass band (GHz)	Component size ($\lambda_g \times \lambda_g$)	Band rejection (GHz)	Return loss (dB)	Insertion loss (dB)	Out of Band suppression (dB)	Fabrication complexity	Filter Type
[5]-I	0 - 9.26	NA	9.3 - 17.67	> 10.3	< 0.5	> 30	easy	LPF (SSPP)
[5]-II	0 - 6.22	NA	6.22 - 11.48	> 10.5	< 0.5	> 50	easy	LPF (SSPP)
[6]	0 - 9.1	6.48×1.00	10 - 12	NA	NA	> 25	easy	LPF (SSPP)
[17]	7.3 - 11.2	4.57×0.91	11.8 - 19.8	> 12	< 2	> 40	difficult	BPF (SSPP-SIW)
[18]	8 - 13.5	1.03×0.71	14.2 - 19.5	> 12	< 1	> 41	difficult	BPF (SSPP-SIW)
[19]	1.19 - 5.43	2.67×0.44	NA	> 10	< 1.9	$> NA$	easy	BPF (SSPP)
[20]	2.1 - 8	1.47×0.42	9 - 20	> 10	< 0.6	> 25	easy	BPF (SSPP)
[21]	1.3 - 6.2	1.00×0.3	9 - 20	> 11	< 1.5	> 20	easy	BPF (SSPP)
This work	0 - 6.77 (sim) 0 - 5 (meas)	0.75×0.12	7.5 - 38 (sim) 8.6 - 38 (meas)	> 15 (sim) > 10 (meas)	< 0.27 (sim) < 1.1 (meas)	> 30 (sim.) > 30 (meas)	easy	LPF (SSPP)

λ_g - guided wavelength at center frequency, NA - not available, sim - simulated, meas - measured.

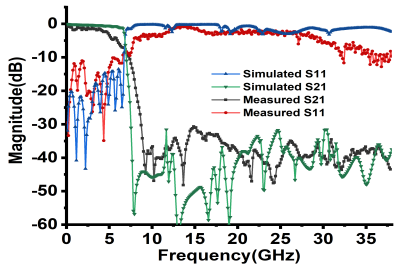

Fig. 13. Simulated and measured S-Parameter graphs

dimensions, low IL, and wide out-of-band suppression characteristics.

V. CONCLUSION

A novel LPF based on SSPP, comprising a tilted slotted stub-shaped unit cell, is proposed to achieve miniaturization and ultra-wide stop-band suppression with high attenuation. The demonstrated LPF showcases enhanced characteristics in electric-field confinement and higher propagation wavenumber when compared to LPFs designed with traditional rectangular trips SSPP cells. The developed LPF measures $61mm \times 10mm$ in overall size. Simulated and experimental results validate the LPF's outstanding passband performance, with an insertion loss of 1.1 dB, a reflection coefficient below -10 dB, and exceptional out-of-band rejection exceeding 30 dB for frequencies over 38 GHz. This compact SSPP LPF holds significant potential for high-performance applications in miniaturized integrated circuits operating within microwave frequency ranges.

REFERENCES

[1] Pendry, J., Martin Moreno, L., Garcia Vidal, F.: Mimicking surface plasmons with structured surfaces. Science. 305(5685), 847–848 (2004)

[2] Tang, Wen Xuan, et al. "Concept, theory, design, and applications of spoof surface plasmon polaritons at microwave frequencies." Advanced Optical Materials 7.1 (2019): 1800421.

[3] Shen X, Cui TJ, Martin-Cano D, Garcia-Vidal FJ. Conformal surface plasmons propagating on ultrathin and flexible films. Proc Natl Acad Sci U S A. 2013 Jan 2;110(1):40-5. doi: 10.1073/pnas.1210417110. Epub 2012 Dec 17. PMID: 23248311; PMCID: PMC3538259.

[4] Ma, H.F., Shen, X., Cheng, Q., Jiang, W.X. and Cui, T.J. (2014), Broadband and high-efficiency conversion from guided waves to spoof surface plasmon polaritons. Laser Photonics Reviews, 8: 146-151. https://doi.org/10.1002/lpor.201300118

[5] S. Lu, K. -D. Xu, Y. -J. Guo and Q. Chen, "Compact Spoof Surface Plasmon Polariton Waveguides With Simple Configurations and Good Performance," in IEEE Transactions on Plasma Science, vol. 49, no. 12, pp. 3786-3792, Dec. 2021.

[6] Ren, B., Zhang, L., Lu, J., Yang, Y., Li, W., Zhang, B. (2021). Compact spoof surface plasmonic waveguide with controllable cutoff frequency and wide stop band. Applied Physics Express, 14(2), 024002.

[7] Xu, K. D., Zhang, F., Guo, Y., Ye, L., Liu, Y. (2019). Spoof surface plasmon polaritons based on balanced coplanar stripline waveguides. IEEE Photonics Technology Letters, 32(1), 55-58.

[8] Wang, M., Sun, S., Ma, H. F., Cui, T. J. (2019). Supercompact and ultrawideband surface plasmonic bandpass filter. IEEE Transactions on Microwave Theory and Techniques, 68(2), 732-740.

[9] Shi Z, Shen Y, Hu S.Spoof surface plasmon polariton transmission line with reduced line-width and enhanced field confinement. Int J RF Microw Comput Aided Eng. 2020;30:e22276. https://doi.org/10.1002/mmce.

[10] Guan, D. F., You, P., Zhang, Q., Xiao, K., Yong, S. W. (2017). Hybrid spoof surface plasmon polariton and substrate integrated waveguide transmission line and its application in filter. IEEE transactions on microwave theory and techniques, 65(12), 4925-4932.

[11] Jidi, L., Cao, X., Gao, J., Li, S., Yang, H., Li, T. (2020). Excitation of odd-mode spoof surface plasmon polaritons and its application on low-pass filters. Applied Physics Express, 13(8), 084004.

[12] Zhang, X., et al (2022). Novel high-efficiency and ultra-compact low-pass filter using double-layered spoof surface plasmon polaritons. Microwave and Optical Technology Letters, 64(6), 1056-1061.

[13] Xu, H., Zhao, W. S., Wang, D. W., Liu, J. (2022). Compact folded SSPP transmission line and its applications in low-pass filters. IEEE Photonics Technology Letters, 34(11), 591-594.

[14] Pang, C., Cao, R. F., Li, L., Liu, H. W. (2023). Spoof Surface Plasmon Polariton Based on Stepped Grooves and Its Application in Compact Low-Pass Filter Design. Plasmonics, 1-11.

[15] Gomaa, W., Smith, L., Shiran, V., Darcie, T. (2020). Terahertz low-pass filter based on cascaded resonators formed by CPS bending on a thin membrane. Optics Express, 28(21), 31967-31978.

[16] Haghighat, M., Darcie, T., Smith, L. (2024). Demonstration of a terahertz coplanar-strip spoof-surface-plasmon-polariton low-pass filter. Scientific Reports, 14(1), 182.

[17] Chen, P., Li, L., Yang, K., Chen, Q. (2018). Hybrid spoof surface plasmon polariton and substrate integrated waveguide broadband band-pass filter with wide out-of-band rejection. IEEE microwave and wireless components letters, 28(11), 984-986.

[18] Sangam, R. S., Kshetrimayum, R. S. (2021). Hybrid spoof surface plasmon polariton and substrate integrated waveguide bandpass filter with high out-of-band rejection for X-band applications. IET Microwaves, Antennas Propagation, 15(3), 289-299.

[19] Zhang, D, et al (2021). Short-circuited stub-loaded spoof surface plasmon polariton transmission lines with flexibly controllable lower out-of-band rejections. Optics Letters, 46(17), 4354-4357.

[20] S. Zhu, P. Wen and Y. Liu, "A Compact Filter Based on Spoof Surface Plasmon Polariton Waveguide for Wide Stopband Suppression," in IEEE Photonics Technology Letters, vol. 34, no. 9, pp. 475-478, 1 May1, 2022.

[21] Ren, B., Qin, C., Guan, X., Xu, K. D. (2023). Compact wideband filter with wide stopband using transition-free spoof surface plasmon polaritons. Journal of Physics D: Applied Physics, 57(3), 035101.